HHS Public Access

Author manuscript

Kidney Int. Author manuscript; available in PMC 2015 March 01.

Published in final edited form as:

Kidney Int. 2014 September ; 86(3): 538–547. doi:10.1038/ki.2014.84.

Deletion of ErbB4 accelerates polycystic kidney disease progression in cpk mice

Fenghua Zeng, **Tomoki Miyazawa**, **Lance A. Kloepfer**, and **Raymond C. Harris**

Division of Nephrology and Hypertension, Department of Medicine, Vanderbilt University School of Medicine, Nashville, Tennessee

Abstract

ErbB4 is highly expressed in the cystic kidneys with polycystic kidney diseases. To investigate its potential role in cystogenesis, *cpk* mice carrying a heart-rescued ErbB4 deletion were generated. Accelerated cyst progression and renal function deterioration were noted as early as 10 days postnatally in *cpk* mice with ErbB4 deletion compared to *cpk* mice, as indicated by increased cystic index, higher kidney weight to body weight ratios and elevated BUN levels. No apparent defects in renal development were noted with ErbB4 deletion itself. Increased cell proliferation was predominately seen in the cortex of cystic kidneys with or without ErbB4 deletion. However, there was significantly more cell proliferation in the cyst-lining epithelial cells in *cpk* mice with ErbB4 deletion. TUNEL staining localized apoptotic cells mainly to the renal medulla. There were significantly more apoptotic cells in the cyst-lining epithelial cells in ErbB4-deleted *cpk* kidneys, with decreased levels of cyclin D1, increased levels of p21, p27 and cleaved caspase 3. Thus, lack of ErbB4 may contribute to elevated cell proliferation and unbalanced cell apoptosis, resulting in accelerated cyst formation and early renal function deterioration. These studies suggest that the high level of ErbB4 expression seen in *cpk* mice may exert relative cytoprotective effects in renal epithelia.

Polycystic kidney diseases (PKD) represent a group of progressive genetic renal disorders that are characterized by the development of numerous fluid filled cysts predominantly in the kidney and liver. There are two major types of hereditary PKDs, autosomal dominant (ADPKD) and autosomal recessive (ARPKD), which together represent the third leading cause of kidney failure in the United States. Compared to ADPKD, ARPKD is a less common, but produces a more severe childhood nephropathy that results in death in 30% of affected infants and end-stage renal disease during the first decade of life in 50% of affected individuals who survive the neonatal period.[1] For this reason, it is important to understand the mechanisms of the cystogenesis to aid in finding new treatment targets to prevent early cyst formation and/or growth. Studies have suggested that dysregulation of epidermal growth factor receptor (EGFR) family members such as EGFR and ErbB2 play a role in the

Correspondence: Dr. Raymond C. Harris, S-3223 Medical Center North, Department of Medicine, Vanderbilt University School of Medicine, Nashville, TN 37232. Tel#: 615-322-2150. Fax #:615-343-2675. ray.harris@vanderbilt.edu.

DISCLOSURES

The authors declare no competing financial interests.

cyst formation in PKD, but the effects of administration of tyrosine kinase inhibitors of EGFR are controversial in different PKD models, ranging from no protective effect to some alleviation of cyst formation.[2,3] On the other hand, the role of ErbB4 in cyst formation remains unclear.

ErbB4, a type I transmembrane receptor tyrosine kinase, belongs to the EGFR superfamily, which consists of four receptors, ErbB1 (EGFR), ErbB2 (Neu), ErbB3, and ErbB4.[4] Among them, only ErbB4 is known to produce functionally distinct isoforms that differ in the extracellular juxtamembrane (JM-a and JM-b) and intracellular cytoplasmic (CYT-1 and CYT-2) domains, as a result of alternative gene splicing. Unlike JM-b, JM-a contains a proteinase cleavage site that can be proteolytically cleaved and generates a membrane-associated 80 kDa fragment that can be degraded by proteasome activity after polyubiquitination or can be further cleaved by γ-secretase to release the intracellular domain (ICD) from the membrane and allow nuclear translocation.[5–7] Unlike CYT-2 ICD, CYT-1 ICD contains an additional 16 amino acids sequence that can serve as binding sites for the phosphatidylinositol 3-OH kinase (PI3K) SH2-domain and for WW-domain containing signaling.[8,9] As a result, CYT-1 ICD is more easily being degraded by ubiquitinyation, while CYT-2 ICD translocates to the nuclei and subsequently promotes cell proliferation.[5,10]

Similar to other members of the EGFR family,[11,12] ErbB4 plays a critical role in embryogenesis, as indicated by gene targeting studies.[13] Mice lacking ErbB4 exhibit defects in cranial neural crest cell migration but die by embryonic day 11 (E11) because of defective heart development.[13] To examine later phenotypes, heart defects were rescued in ErbB4 mutant mice by expressing ErbB4 under a cardiac-specific myosin promoter.[14] Rescued ErbB4 mutant ($ErbB4^{del}ht^{+}$) mice reach adulthood and are fertile. The abnormalities found in $ErbB4^{del}ht^{+}$ mice include aberrant cranial nerve architecture, increased numbers of large interneurons within the cerebellum, defects in mammary lobuloalveolar differentiation and failure of lactation.[14] To our knowledge, the influence of ErbB4 deletion on kidney development and renal function in $ErbB4^{del}ht^{+}$ mice has not been reported; however, conditional knock-out of ErbB4 in the kidneys resulted in abnormal kidney histological features such as dilated collecting ducts and tubular epithelial cell mispolarization.[15] On the other hand, ErbB4 was found upregulated in the cystic kidneys of *bpk* mice, a murine ARPKD model, and ErbB4 overexpression in the mouse kidneys promoted formation of cortical tubular cysts.[15,16] To clarify the potential role of ErbB4 in cyst formation, in the current study, we deleted ErbB4 in *cpk* mice, another murine ARPKD model, by crossing $ErbB4^{del}ht^{+}$ with *cpk* mice. Surprisingly, we found that ErbB4 deletion accelerated cyst progression and renal function decline in *cpk* mice, which indicated that the high levels of ErbB4 in *cpk* mice during the cyst formation may have protective effects rather than contribute to the cyst formation.

RESULTS

No apparent defects in the renal development of mice with ErbB4 deletion

Heart excluded ErbB4 deletion was confirmed by Western blots using tissue lysate extracted from heart, kidney, liver, and brain of E15 mice, at a time when ErbB4 is highly expressed

in kidneys.[17] As expected, the expression of ErbB4 was deleted from kidneys as well as other organs such as the brain, but expression was maintained in the heart, albeit at a somewhat lower level than in wild-type (Figure 1a and b). Heart excluded ErbB4 deletion was also confirmed at the mRNA level by RT-PCR as originally described (Figure 1c).[14] Both we and others have shown that ErbB4 is expressed in the ureteric buds during renal development and its derivative tubules in adult kidneys, which indicates that ErbB4 may play a role in renal development.[15,17] To rule out possible development defects caused by ErbB4 deletion, renal morphology, nephron numbers and renal function were investigated. The results showed that compared to controls, no apparent tubular dilatation or other renal morphology changes were detected in the kidneys with ErbB4 deletion (Figure 1d). No significant changes in renal function were assessed by BUN levels (Figure 1e). We also examined nephron numbers in adult mice at 8 weeks of age, when both nephrogenesis and kidney growth are completed. The results showed that mice with ErbB4 deletion have slightly lower numbers of nephron (15944 ± 1907, n = 10) compared to control (16462 ± 1297, n = 9), but no statistically difference was detected ($P = 0.2316$) (Figure 1f).

High levels of ErbB4 were expressed in the cyst-lining epithelial cells of *cpk* kidneys

To investigate the expression levels of ErbB4 in *cpk* mice, tissue lysates of whole kidneys of age (postnatal 18, P18) and sex-matched (male) wild-type and *cpk* mice were used for immunoblots. ErbB4 expression levels were significantly higher in *cpk* kidneys compared to wild-type, with a 180 kDa band, which represents the full-length ErbB4 protein, and an 80 kDa band, which represents ErbB4 ICD (Figure 2a upper panel and b). The presence of high levels of ErbB4 ICD indicated that ErbB4 was actively cleaved in the kidneys of *cpk* mice. This cleavage can be induced by ErbB4 activation through the binding of ligands to ErbB4.[18] Indeed, high levels of ErbB4 phosphorylation were detected in the kidneys of *cpk* mice compared to wild-type (Figure 2a middle panel and c). At the same stage, the expression levels of HB-EGF, a ligand that can bind to both EGFR and ErbB4, were also increased in *cpk* kidneys compared to wild-type (Figure 2d and e), which may contribute to the high levels of ErbB4 activation and its cleavage. The results from immunostaining showed that strong ErbB4 immunoreactivity was localized to the cyst-lining epithelial cells in the kidneys of *cpk* mice, while only minimum level of ErbB4 was detected in wild-type at the same age (Figure 2f). At this stage of *cpk* mice (P18), most of the cysts were derived from collecting ducts (CDCs), although minimum cysts from proximal tubules (PTCs) still exist. By double-immunofluorescence staining with either dolichos biflorus agglutinin (DBA), a marker for collecting ducts, or lotus tetragonolobus lectin (LTL), a marker for proximal tubules, we were able to locate ErbB4 to the epithelial cells of CDCs, not in PTCs or non-cystic proximal tubules (Figure 3), which was consistent with the normal ErbB4 tubular expression pattern.[17]

ErbB4 deletion in *cpk* mice accelerated kidney cyst progression and renal function deterioration

To investigate the role of ErbB4 in cystic disease, heterozygous $ErbB4^{del}ht^{+}$-*cpk*/+ mice were bred to generate mice homozygous for both genes ($ErbB4^{del}ht^{+}$-*cpk*). $ErbB4^{del}ht^{+}$-*cpk* mice have a shorter life-span compared to *cpk* mice. Death occurred on P15 and P21 on average in $ErbB4^{del}ht^{+}$-*cpk* and *cpk* mice, respectively ($P < 0.0001$ by log-rank test; Figure

4a). Therefore, P10 mice were used in the following studies. Grossly, all cystic kidneys were larger than non-cystic controls, with *ErbB4*^{del}*ht*$^{+}$*-cpk* mice having the largest kidneys (Figure 4b). Kidney size was quantified by kidney planar surface area on photographed kidneys and by kidney weight to body weight ratios. By both measurements, kidneys from *ErbB4*^{del}*ht*$^{+}$*-cpk* mice were significantly larger than from *cpk* mice, with no difference between *ErbB4*^{del}*ht*$^{+}$ and wild-type mice (Figure 4c and d). Morphologically, severe cyst formations, indicated by remnant cortical structures and higher cystic index, which represent the percentage of total area occupied by cysts, were seen in *ErbB4*^{del}*ht*$^{+}$*-cpk* kidneys compared to *cpk* kidneys (Figure 4e and f). Renal function was assessed by BUN levels. All *cpk* mice had higher BUN levels than non-*cpk* mice, and ErbB4 deletion further increased BUN levels compared to *cpk* only mice (Figure 4g).

ErbB4 deletion in *cpk* mice increased renal cortex cell proliferation in the cyst-lining epithelial cells

To investigate the cellular mechanism related to the severe cyst progression in *cpk* mice with ErbB4 deletion, cell proliferation, a key feature of cyst growth, was assessed by both BrdU and Ki67 staining. BrdU was injected 4 hours before sacrifice and BrdU staining was carried out as described in the methods. Overall, there were more proliferating cells in the cortex compared to the medulla in the kidneys of *cpk* and *ErbB4*^{del}*ht*$^{+}$*-cpk* mice (Figure 5a), while no significant differences were detected in the cortex of wild-type and *ErbB4*^{del}*ht*$^{+}$ mice (Supplementary Figure S1). *ErbB4*^{del}*ht*$^{+}$*-cpk* mice exhibited higher number of BrdU positive cells in the cortical cysts and less BrdU positive cells in the medullary cysts compared to *cpk* mice (Figure 5a and b). To further investigate whether the proliferating cells were lining cysts of collecting duct origin, Ki67, a nuclear protein complex expressed in the G1, S, G2 and M phases of the cell cycle of proliferating cells, was used for double immunoflouroscence staining with DBA. The results showed the same pattern as BrdU staining, with more Ki-67 positive cells located in the cortex compared to the medulla in both *ErbB4*^{del}*ht*$^{+}$*-cpk* mice and *cpk* mice. Compared to *cpk* kidneys, significantly more Ki67 positive cells were cyst-lining epithelial cells of collecting duct origin in *ErbB4*^{del}*ht*$^{+}$*-cpk* kidneys (Figure 5c and d). Those results suggested that increased cyst-lining epithelial cell proliferation may be related to the accelerated cyst progression in the *ErbB4*^{del}*ht*$^{+}$*-cpk* mice.

ErbB4 deletion in *cpk* mice increased renal medullary cell apoptosis in the cyst-lining epithelial cells

Consistent with an acceleration of cyst progression in the kidneys of *ErbB4*^{del}*ht*$^{+}$*-cpk* mice, we observed an increase in TUNEL labeling in the cyst-lining epithelial cells of *ErbB4*^{del}*ht*$^{+}$*-cpk* kidneys compared to *cpk* kidneys ($P < 0.05$). At P10, only minimal TUNEL positive cells were seen in the cystic kidneys of *cpk* mice. In contrast to the distribution pattern of cell proliferation markers BrdU and Ki67, most of the TUNEL positive cells were found in the medulla compared to the cortex (Figure 6a and b).

Previous studies have shown that ErbB4 ICD can function as a nuclear chaperone for signal transducer and activator of transcription 5A (STAT5A) to promote the expression of cyclin D1, a cell cycle regulator that promotes cell cycle progression through the G1-S phase.[19–21] To investigate the role of cell cycle regulation related to ErbB4 deletion, cyclin D1 and its

related signaling pathway were studied. The results showed that compared to *cpk* kidneys, the expression levels of cyclin D1 was significantly decreased in the kidneys of *ErbB4^{del}ht^{+}-cpk* mice. By immunochemistry, this reduction was mainly found in the medulla compared to the cortex (Supplementary Figure S2). Concomitantly, levels of cyclin-dependent kinase inhibitor proteins (CIP/KIP), p21^{cip} and p27^{kip}, were increased in the kidneys of *ErbB4^{del}ht^{+}-cpk* mice (Figure 7a and b). These results suggested that decreased cell cycle progression may contribute to the high apoptotic levels in *ErbB4^{del}ht^{+}-cpk* mice, which were also indicated by its increased levels of apoptotic executor, cleaved caspase 3 (Figure 7a and b).

ErbB4 deletion in *cpk* mice increased renal fibrosis

As ErbB4 deletion has been shown to increase fibrosis in other organs, such as lung,[22] we investigated whether fibrosis also played a role in ErbB4 deleted cystic kidneys. Renal fibrosis was assessed by picosirius red staining. The results showed that at P10, picosirius red staining was only seen in the peri-vascular area in the kidneys of either wild-type or *ErbB4^{del}ht^{+}* mice. Slightly increased picosirius red staining was seen in *cpk* kidneys, with no significant difference compared to non-cystic controls. In contrast, there was a marked increase in picosirius red staining areas located in the parenchyma between the cysts in *ErbB4^{del}ht^{+}-cpk* kidneys (Figure 8a and b).

DISCUSSION

Unlike other members in the ErbB family, the role of ErbB4 in the cyst formation is unknown. In the current study, we demonstrated that ErbB4 deletion in *cpk* mice, a murine ARPKD model, promoted cyst formation and accelerated renal function decline.

Previous studies have shown that ErbB4 is highly expressed in the developing ureteric bud, which generates the collecting-duct cells and the ureters, suggesting a role for ErbB4 in the development of kidney epithelium.[15,17] To exclude the cyst-promoting effect from ErbB4 deletion itself, detailed studies were performed and no apparent renal development defects were detected. It has been reported that conditional ErbB4 loss-of-function under the pax8 promoter produced larger duct lumens in the adulthood.[15] However, no obvious tubular dilatation or cyst formation and no significant renal function changes were detected in our studies. Those differences may be related to the genetic background of the mouse strain, as seen with EGFR deletion.[23] *ErbB4^{del}ht^{+}* mice used in our experiments are on the C57BL/6J and FVB mixed background, which may increase resistance to renal injury.[24]

Similar to the previous report in *bpk* mice,[16] high ErbB4 expression levels were detected in *cpk* mice, another murine ARPKD model, which makes it a good model to study the role of ErbB4 in the cyst formation. In *cpk* mice, the cysts evolve in three main stages. Stage I (P1 to P6) consists of segmental dilatations of both proximal and collecting tubules; in stage II (P7–P13), the collecting duct cysts (CDCs) undergo rapid growth; and in stage III (after P13), almost all the cysts are CDCs and the nephrons are located only in the outer cortex between the cysts.[25] Many *cpk* mice die around P21. Our studies showed that many *cpk* mice with ErbB4 deletion died around P15 instead of P21, which indicated that ErbB4 deletion accelerated cyst progression in *cpk* mice.

Abundant studies have linked enhanced cell proliferation and unbalanced cell death in tubular epithelial cells to the cyst formation in different PKD models. (see the excellent review by Goilav B.[26]) By using in vivo BrdU labeling and Ki67 immunostaining, significantly more proliferating cells were located in the cyst-lining epithelial cells (CLEC) in the thin cortex area in *ErbB4*^{del}*ht*$^{+}$*-cpk* mice compared to *cpk* mice, while the opposite pattern was detected in the medulla, with more proliferating cells in CLEC in *cpk* mice compared to *ErbB4*^{del}*ht*$^{+}$*-cpk* mice. On the other hand, more apoptotic cells were found in the medullary CLEC in *ErbB4*^{del}*ht*$^{+}$*-cpk* kidneys compared to *cpk* kidneys. The disparity in the cell proliferation and apoptosis status in the cortex and medulla may stem from the different biological properties of the ErbB4 isoforms and their distinct localization in the kidney. Even though both JM-a/CYT-1 and JM-a/CYT-2 are expressed in the kidneys, their distributions are not the same. JM-a/CYT-1 is mainly localized to the cortex while JM-a/CYT-2, the predominant isoform of ErbB4 in the kidney, is mainly localized in the medulla.[17] While both isoforms are cleavable and release ICD to the cytoplasm, signaling differences between CYT-1 ICD and CYT-2 ICD have been previously reported. For example, levels of kinase activity, protein stability, and nuclear accumulation are greater for CYT-2 ICD than for CYT-1 ICD.[5,27] As a result, CYT-1 ICD inhibits cell proliferation, but promotes cell differentiation. CYT-2 ICD promotes cell proliferation and inhibits cell differentiation.[28] Thus, deletion of JM-a/CYT-1, the main isoform of ErbB4 in the renal cortex, would be expected to remove the inhibitory effect of cell proliferation. As a result, cells lining the cortical collecting duct would proliferate more. On the other hand, deletion of JM-a/CYT-2, the main isoform of ErbB4 in the renal medulla, may decrease cell proliferation or even promote cell apoptosis.

On the other hand, high levels of ErbB4 CYT-2 in mammalian epithelial cells promoted cell proliferation concomitant with increased cyclin D1 expression.[28] Our earlier study also indicated that high levels of cyclin D1 contributed to the renal epithelial repair after acute kidney injury.[29] In this study, we found that cyclin D1 levels were decreased in the kidneys of ErbB4 deletion *cpk* mice compared to *cpk* mice, which may contributed to its increased level of apoptosis.

Renal fibrosis, a feature commonly found in human polycystic kidneys, was evident in ErbB4 deleted cystic kidneys, while no obvious fibrosis was detected in *cpk* kidneys at this stage (P10). Even though studies have shown that ErbB4 deletion can cause fibrosis in other organs,[22] no apparent renal fibrosis was detected in ErbB4 deletion mouse kidneys at the age they were studied. We speculate that ErbB4 deletion on the genetic *cpk* mutation background promoted the fibrosis formation, along with other insults such as increased proliferation and non-balanced apoptosis, results in progressive renal failure and early death. Those data may be confounded by the fact that those mice were generated on mixed genetic backgrounds. To minimize this limitation, only the littermates from the same founder were used for comparison.

In summary, we demonstrate that ErbB4 deletion in *cpk* mice accelerated cyst formation and renal function decline by promoting fibrosis formation, increasing cyst-lining epithelial cell proliferation in the cortex and elevating cell apoptosis in the medulla. These findings suggest that the upregulation of ErbB4 expression seen in *cpk* mice may reflect the response

of epithelial cells to stress,[30] and consequently exert cytoprotective effects in renal epithelia. This cytoprotective effects may play an important role before P10, when a critical renal developmental switch occurs.[31] Studies have shown that EGF administration during P2 to P9 ameliorated cyst progression in *cpk* mice and it was proposed that the neonatal EGF or EGF-like activity prior to P10 may play a role in epithelial differentiation.[32,33] Therefore, in the treatment of polycystic kidney disease, both the timing and the specificity of the EGFR tyrosine kinase inhibitors should be considered.

MATERIALS AND METHODS

Animal care, breeding and genotyping

Animals were housed at the Vanderbilt Medical Center veterinary facility. Animal care and all experimental protocols in our studies complied with the regulations of and were approved by Vanderbilt University's Institutional Animal Care and Usage Committee. C57BL/6J(B6)/FVB mice with ErbB4 deletion that was rescued from their lethal cardiac defects by expressing human ErbB4 cDNA under the cardiac-specific myosin heavy chain (MHC) promoter (*ErbB4*$^{-/-}$*ht*$^{+}$) were kindly provided by Dr. Frank E. Jones (Department of Cell and Molecular Biology, Tulane University, New Orleans, LA) in agreement with Dr. Martin Gassmann (Department of Biomedicine, Institute of Physiology, University of Basel, Switzerland).[14] B6 mice containing the *cpk* mutant gene, heterozygous Cys1$^{cpk/+}$ (*cpk*/+) mice, were purchased from Jackson Laboratory (Bar Harbor, ME). *ErbB4*$^{-/-}$*ht*$^{+}$ mice were crossed with *cpk* mice to generate *ErbB4*$^{-/+}$*ht*$^{+}$-cpk/+ mice (B6/FVB), which were intercrossed to generate *ErbB4*$^{-/-}$*ht*$^{+}$-*cpk*/+ (*ErbB4*^{del}*ht*$^{+}$-*cpk*/+) or *cpk*/+ mice and were used for the final breeding. All the mice analyzed were on the same B6 and FVB mixed genetic background. Genotypes were performed by PCR using primers as previously reported.[14]

Antibodies and reagents

5-Bromo-2′-Deoxyuridine (BrdU), collagenase, and anti-β-actin antibody were purchased from Sigma-Aldrich (St. Louis, MO); TdT In Situ Apoptosis Detection Kit (Fluorescein) was from R&D systems (Minneapolis, MN); Dynabeads were from Invitrogen (Grand Island, NY); anti-Ki67 antibody was from Abcam (Cambridge, MA); antibodies for HB-EGF (E-10), ErbB4 (c-18), cyclin D1 (H295) and p21(C19) were from Santa Cruz Biotechnology (Santa Cruz, CA); antibodies for phospho-HER4/ErbB4 (Tyr1284), cleaved caspase 3, and p27 Kip1 were from Cell Signaling Technology (Beverly, MA); fluorescein labeled LTL, fluorescein labeled DBA, and avidin-biotin complex (ABC) kits were from VectorLabs (Burlingame, CA).

Unless otherwise noted, antibodies were used at 1:200 for immunostaining and 1:1000 for Western blots.

Glomeruli isolation and quantitation of nephron number

Glomeruli were isolated as previously prescribed,[34] with modifications. 8-week old male littermates with *ErbB4*^{del}*ht*$^{+}$ or wild-type were anesthetized and perfused through the heart with 8×10^{7} dynabeads diluted in 40 ml Hanks Buffered Saline Solution (HBSS). The

kidneys were removed and digested in collagenase (1 mg/ml) containing 100 U/ml deoxyribonuclease I in HBSS at 37°C for 30 minutes with gentle agitation. The collagenase-digested tissue was pressed through a 100 μm cell strainer using a pestle and washed with HBSS. The cell suspension was centrifuged at 200 x *g* for 5 minutes. The cell pellet with the glomeruli containing dynabeads was resuspended in HBSS, harvested by a Magnetic Particle Concentrator, washed with HBSS and fixed in 4% paraformaldehyde (PFA) overnight at 4°C before counting in a blinded fashion using a microscope.

Measurement of blood urea nitrogen (BUN)

Mice were euthanized at the indicated ages. Before removing the kidneys, blood was collected by intracardiac puncture and centrifuged at 2000 x g for serum collection. BUN levels were determined using the QuantiChrom™ Urea Assay Kit (DIUR-500) (BioAssay Systems, Hayward, CA).

Renal histopathology and immunostaining

At indicated ages, mice were euthanized and kidneys removed, weighed, photographed and then fixed in 4% PFA before paraffin embedding. 5 μm midsagittal sections were stained with hemotoxylin and eosin (H&E) or used for immunostaining as previously described.[17] The images were examined using a Zeiss microscope (Thornwood, NY). Cystic index was determined and reported as the percentage of total area occupied by cysts, as previously described.[35]

BrdU immunohistochemistry

P10 mice received one intraperitoneal 100 mg/kg injection of 10 mg/ml BrdU. Four hours after the administration of BrdU, mice were transcardially perfused under deep anesthesia with heparinized saline followed by 4 % PFA. Kidneys were removed, decapsulized, and postfixed overnight in fresh 4% PFA at 4°C. 5 μm paraffin sections were used for BrdU staining using BrdU In-Situ Detection Kit (BD Biosciences, San Jose, CA) following manufacturer's instructions. The number of BrdU positive cells per high power (HP) field was counted using ImageJ software under 200 x magnification.[36]

TUNEL staining

Staining for the presence of apoptotic cells was completed using the TdT In Situ Apoptosis Detection Kit (Fluorescein) according to the manufacturer's recommendations. Following rehydration, sections were incubated with proteinase K solution for 20 minutes at room temperature. After equilibration with TdT labeling buffer, sections were incubated in TdT labeling reaction mix for 1 hour at 37°C. The reaction was stopped by immersing the sections into TdT stop buffer, and TdT labeling was detected by incubating with strep-fluor solution.

Immunoblot

A quarter of the kidney was snap-frozen and stored at −80°C until use. Frozen samples were homogenized and lysed in ice-cold TGH buffer as previously described.[17] For detection of cyclin D1, p21, p27, cleaved caspase 3, and TATA binding protein (TBP), nuclear proteins

were extracted using NE-PER nuclear and cytoplasmic extraction reagents (Thermo Scientific, Rockford, IL) following the manufacturer's instructions. Western blots were carried out as previously described.[17]

Statistics

Data were evaluated using unpaired t-test for two groups and ANOVA followed by a post Bonferroni's multiple comparison test for three or more groups. Values were expressed as means ± SE for at least three separate experiments. $P < 0.05$ was considered statistically significant.

Supplementary Material

Refer to Web version on PubMed Central for supplementary material.

Acknowledgments

This work was supported by National Institutes of Health Grants DK38226, DK51265, DK62794, DK095785 (R.C.H) and funds from the Department of Veterans Affairs.

References

1. Wilson PD, Goilav B. Cystic disease of the kidney. Annu Rev Pathol. 2007; 2:341–368. [PubMed: 18039103]
2. Orellana SA, Sweeney WE, Neff CD, et al. Epidermal growth factor receptor expression is abnormal in murine polycystic kidney. Kidney Int. 1995; 47:490–499. [PubMed: 7723235]
3. Torres VE, Sweeney WE Jr, Wang X, et al. Epidermal growth factor receptor tyrosine kinase inhibition is not protective in PCK rats. Kidney Int. 2004; 66:1766–1773. [PubMed: 15496147]
4. Olayioye MA, Neve RM, Lane HA, et al. The ErbB signaling network: receptor heterodimerization in development and cancer. EMBO J. 2000; 19:3159–3167. [PubMed: 10880430]
5. Zeng F, Xu J, Harris RC. Nedd4 mediates ErbB4 JM-a/CYT-1 ICD ubiquitination and degradation in MDCK II cells. FASEB J. 2009; 23:1935–1945. [PubMed: 19193720]
6. Ni CY, Murphy MP, Golde TE, et al. gamma -Secretase cleavage and nuclear localization of ErbB-4 receptor tyrosine kinase. Science. 2001; 294:2179–2181. [PubMed: 11679632]
7. Vecchi M, Carpenter G. Constitutive proteolysis of the ErbB-4 receptor tyrosine kinase by a unique, sequential mechanism. J Cell Biol. 1997; 139:995–1003. [PubMed: 9362517]
8. Komuro A, Nagai M, Navin NE, et al. WW domain-containing protein YAP associates with ErbB-4 and acts as a co-transcriptional activator for the carboxyl-terminal fragment of ErbB-4 that translocates to the nucleus. J Biol Chem. 2003; 278:33334–33341. [PubMed: 12807903]
9. Carpenter G. ErbB-4: mechanism of action and biology. Exp Cell Res. 2003; 284:66–77. [PubMed: 12648466]
10. Junttila TT, Sundvall M, Lundin M, et al. Cleavable ErbB4 isoform in estrogen receptor-regulated growth of breast cancer cells. Cancer Res. 2005; 65:1384–1393. [PubMed: 15735025]
11. Erickson SL, O'Shea KS, Ghaboosi N, et al. ErbB3 is required for normal cerebellar and cardiac development: a comparison with ErbB2-and heregulin-deficient mice. Development. 1997; 124:4999–5011. [PubMed: 9362461]
12. Miettinen PJ, Berger JE, Meneses J, et al. Epithelial immaturity and multiorgan failure in mice lacking epidermal growth factor receptor. Nature. 1995; 376:337–341. [PubMed: 7630400]
13. Gassmann M, Casagranda F, Orioli D, et al. Aberrant neural and cardiac development in mice lacking the ErbB4 neuregulin receptor. Nature. 1995; 378:390–394. [PubMed: 7477376]

14. Tidcombe H, Jackson-Fisher A, Mathers K, et al. Neural and mammary gland defects in ErbB4 knockout mice genetically rescued from embryonic lethality. Proc Natl Acad Sci U S A. 2003; 100:8281–8286. [PubMed: 12824469]
15. Veikkolainen V, Naillat F, Railo A, et al. ErbB4 modulates tubular cell polarity and lumen diameter during kidney development. J Am Soc Nephrol. 2012; 23:112–122. [PubMed: 22076439]
16. Nemo R, Murcia N, Dell KM. Transforming growth factor alpha (TGF-alpha) and other targets of tumor necrosis factor-alpha converting enzyme (TACE) in murine polycystic kidney disease. Pediatr Res. 2005; 57:732–737. [PubMed: 15774823]
17. Zeng F, Zhang MZ, Singh AB, et al. ErbB4 isoforms selectively regulate growth factor induced Madin- Darby canine kidney cell tubulogenesis. Mol Biol Cell. 2007; 18:4446–4456. [PubMed: 17761534]
18. Zhou W, Carpenter G. Heregulin-dependent trafficking and cleavage of ErbB-4. J Biol Chem. 2000; 275:34737–34743. [PubMed: 10944525]
19. Lukas J, Bartkova J, Bartek J. Convergence of mitogenic signalling cascades from diverse classes of receptors at the cyclin D-cyclin-dependent kinase-pRb-controlled G1 checkpoint. Molecular and cellular biology. 1996; 16:6917–6925. [PubMed: 8943347]
20. Lange CA, Richer JK, Shen T, et al. Convergence of progesterone and epidermal growth factor signaling in breast cancer. Potentiation of mitogen-activated protein kinase pathways. J Biol Chem. 1998; 273:31308–31316. [PubMed: 9813039]
21. Williams CC, Allison JG, Vidal GA, et al. The ERBB4/HER4 receptor tyrosine kinase regulates gene expression by functioning as a STAT5A nuclear chaperone. J Cell Biol. 2004; 167:469–478. [PubMed: 15534001]
22. Purevdorj E, Zscheppang K, Hoymann HG, et al. ErbB4 deletion leads to changes in lung function and structure similar to bronchopulmonary dysplasia. Am J Physiol Lung Cell Mol Physiol. 2008; 294:L516–522. [PubMed: 18203811]
23. Threadgill DW, Dlugosz AA, Hansen LA, et al. Targeted disruption of mouse EGF receptor: effect of genetic background on mutant phenotype. Science. 1995; 269:230–234. [PubMed: 7618084]
24. Ma LJ, Fogo AB. Model of robust induction of glomerulosclerosis in mice: importance of genetic background. Kidney Int. 2003; 64:350–355. [PubMed: 12787428]
25. Ojeda JL. Abnormal tenascin expression in murine autosomal recessive polycystic kidneys. Nephron. 1999; 82:261–269. [PubMed: 10395999]
26. Goilav B. Apoptosis in polycystic kidney disease. Biochim Biophys Acta. 2011; 1812:1272–1280. [PubMed: 21241798]
27. Sundvall M, Peri L, Maatta JA, et al. Differential nuclear localization and kinase activity of alternative ErbB4 intracellular domains. Oncogene. 2007; 26:6905–6914. [PubMed: 17486069]
28. Muraoka-Cook RS, Sandahl MA, Strunk KE, et al. ErbB4 splice variants Cyt1 and Cyt2 differ by 16 amino acids and exert opposing effects on the mammary epithelium in vivo. Molecular and cellular biology. 2009; 29:4935–4948. [PubMed: 19596786]
29. Howard C, Tao S, Yang HC, et al. Specific deletion of glycogen synthase kinase-3beta in the renal proximal tubule protects against acute nephrotoxic injury in mice. Kidney Int. 2012; 82:1000–1009. [PubMed: 22785175]
30. Menon V, Rudym D, Chandra P, et al. Inflammation, oxidative stress, and insulin resistance in polycystic kidney disease. Clin J Am Soc Nephrol. 2011; 6:7–13. [PubMed: 20829421]
31. Piontek K, Menezes LF, Garcia-Gonzalez MA, et al. A critical developmental switch defines the kinetics of kidney cyst formation after loss of Pkd1. Nat Med. 2007; 13:1490–1495. [PubMed: 17965720]
32. Gattone VH 2nd, Lowden DA, Cowley BD Jr. Epidermal growth factor ameliorates autosomal recessive polycystic kidney disease in mice. Dev Biol. 1995; 169:504–510. [PubMed: 7781894]
33. Gattone VH 2nd, Calvet JP. Murine infantile polycystic kidney disease: a role for reduced renal epidermal growth factor. Am J Kidney Dis. 1991; 17:606–607. [PubMed: 1710422]
34. Takemoto M, Asker N, Gerhardt H, et al. A new method for large scale isolation of kidney glomeruli from mice. Am J Pathol. 2002; 161:799–805. [PubMed: 12213707]

35. Cao Y, Semanchik N, Lee SH, et al. Chemical modifier screen identifies HDAC inhibitors as suppressors of PKD models. Proc Natl Acad Sci U S A. 2009; 106:21819–21824. [PubMed: 19966229]

36. Schneider CA, Rasband WS, Eliceiri KW. NIH Image to ImageJ: 25 years of image analysis. Nat Methods. 2012; 9:671–675. [PubMed: 22930834]

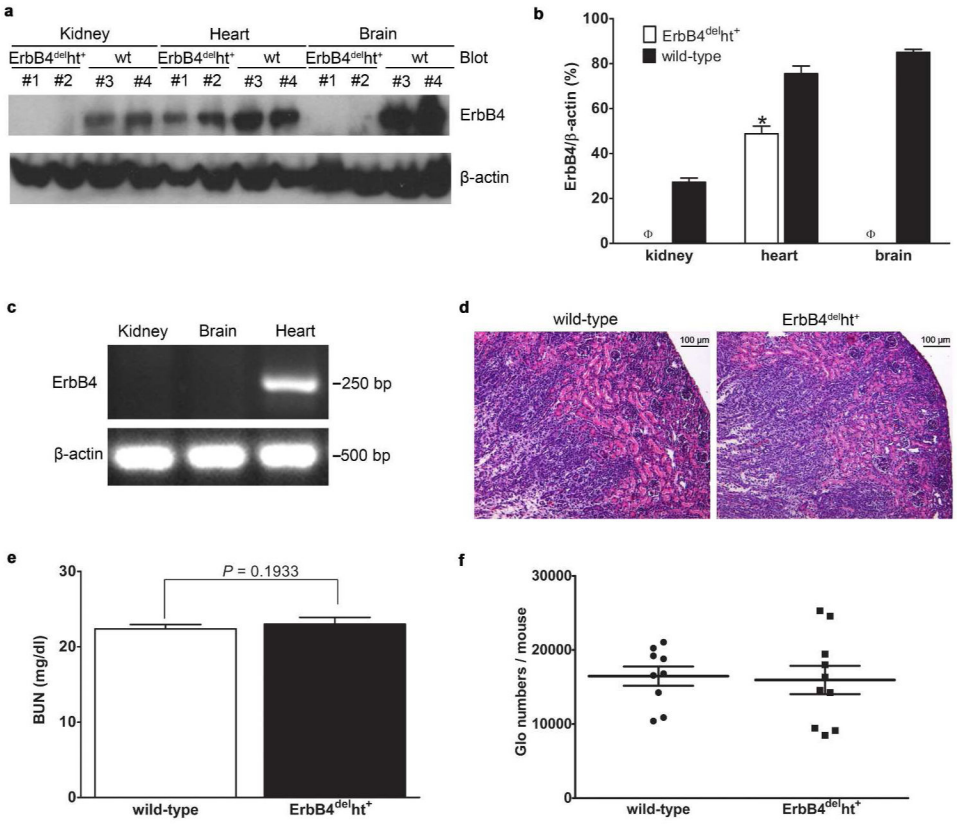

Figure 1.

ErbB4 deletion in the kidneys of *ErbB4*^{del}*ht*$^{+}$ mice. (**a**) ErbB4 deletion in *ErbB4*^{del}*ht*$^{+}$ mice was confirmed by Western blots using an anti-ErbB4 antibody. wt: wild-type. (**b**) Densitometric analysis of the Western blot bands of ErbB4 in (a) and expressed as ErbB4/β-actin. **P* < 0.05, $^{\varphi}$*P* < 0.001 compared to wild-type. (**c**) Heart excluded ErbB4 mRNA deletion was confirmed by RT-PCR. β-actin mRNA was used as a positive control. (**d**) Representative H&E staining of P10 kidneys from wild-type and *ErbB4*^{del}*ht*$^{+}$ mice. n = 10 in each group. No apparent tubular dilatation or cyst formation was detected. (**e**) No significant difference of BUN levels between wild-type and *ErbB4*^{del}*ht*$^{+}$ mice. n = 10 to 15 in each group. (**f**) Glomerular (Glo) numbers were calculated on adult mice and no significant differences were detected between wild-type and *ErbB4*^{del}*ht*$^{+}$ mice. n = 9 to 10 in each group.

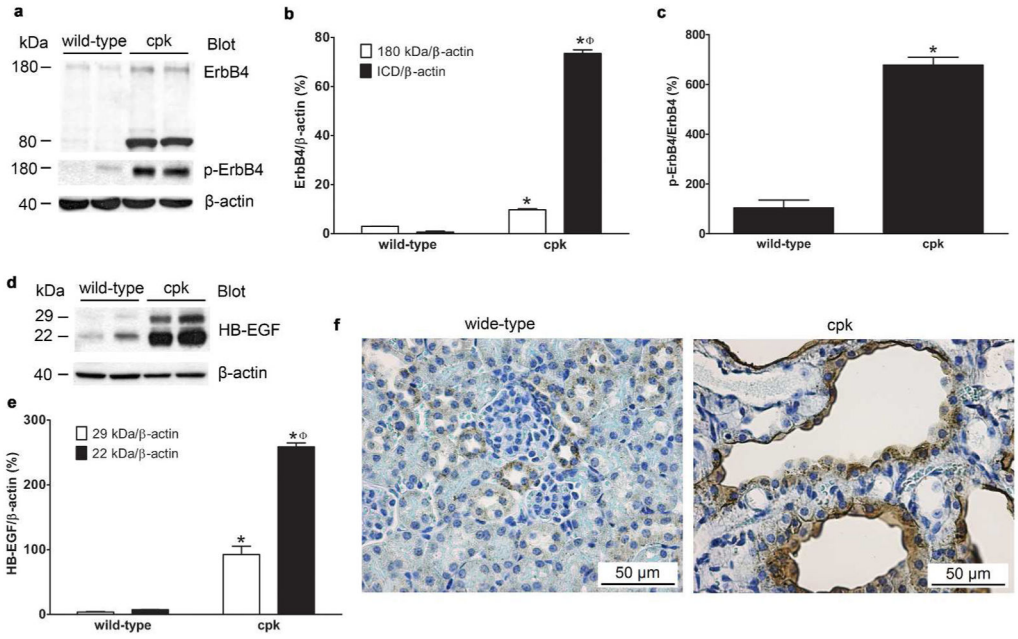

Figure 2.

ErbB4 expression levels. (**a**) Elevated levels of ErbB4 expression levels, both full-length (180 kDa) and intracellular domain (80 kDa, ICD), and increased phosphorylation levels of the full length ErbB4 were detected in the kidneys from *cpk* mice compared to the kidneys from wild-type mice. Equal amount of protein loading was confirmed by β-actin blots. (**b**) Densitometric analysis of the Western blot bands of ErbB4 in (a) and expressed as ErbB4/β-actin. Compared to the 180 kDa full-length ErbB4, significant levels of ICD were detected in *cpk* mice. **P* < 0.05 compared to wild-type. $^{\varphi}P$ < 0.05 compared to 180 kDa full-length ErbB4. (**c**) Densitometric analysis of the Western blot bands of phosphor-ErbB4 in (a) and expressed as p-ErbB4/β-actin. **P* < 0.05. (**d**) Elevated levels of HB-EGF expression in *cpk* kidneys. The expression levels of both pro-HB-EGF (29 kDa) and mature HB-EGF (22 kDa) were increased in *cpk* kidneys compared to wild-type. (**e**) Densitometric analysis of the Western blot bands in (d) and expressed as HB-EGF/β-actin. **P* < 0.05 compared to wild-type. $^{\varphi}P$ < 0.05 compared to 29 kDa pro-HB-EGF. In (b), (c) and (e), values represent mean ± SE of at least three independent experiments. (**f**) Increased ErbB4 immunoreactivity (brown) was seen in cyst-lining epithelial cells in *cpk* kidneys compared to wild-type.

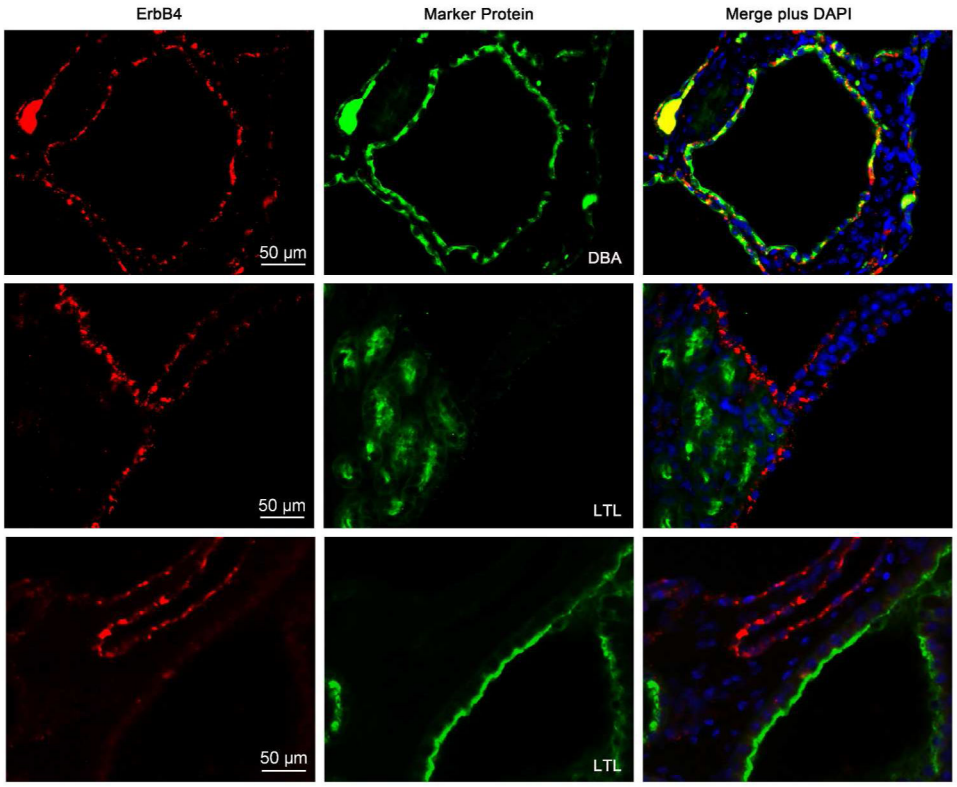

Figure 3.

Double immunofluorescence staining of ErbB4 and tubular marker protein in P18 *cpk* kidneys. ErbB4 (red) was colocalized with DBA (green), a collecting ducting marker. No colocalization with LTL (green), a proximal tubular marker. Nuclei were stained with DAPI (blue).

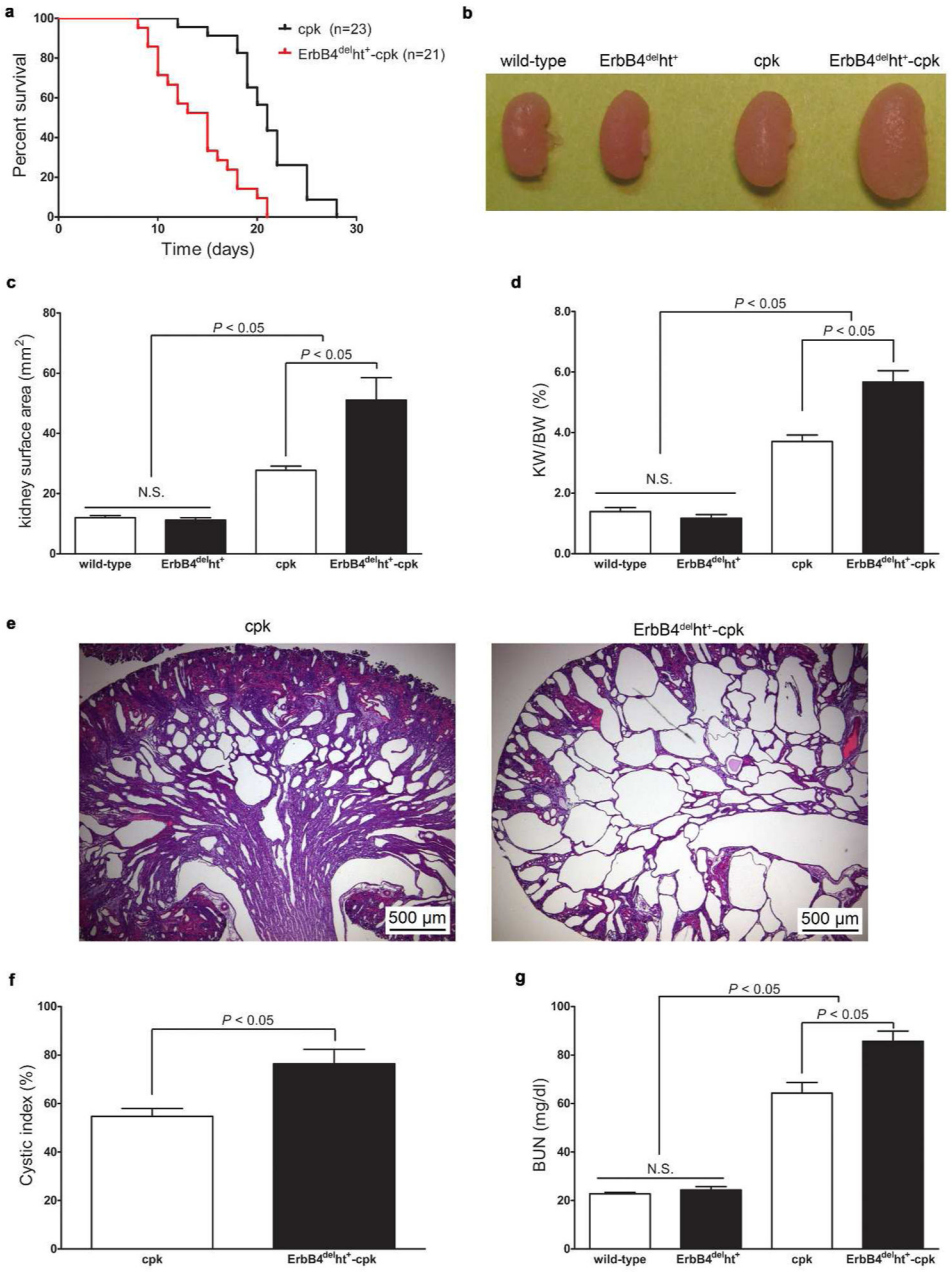

Figure 4.

ErbB4 deletion in cystogenesis. (**a**) Kaplan-Meier survival curve of *ErbB4*^{del}*ht*$^{+}$*-cpk* and *cpk* mice followed until the time of death. (**b**) Grossly, enlarged kidneys were seen in *ErbB4*^{del}*ht*$^{+}$*-cpk* mice compared to *cpk* mice. No significant difference (N.S.) was seen between the kidneys from *ErbB4*^{del}*ht*$^{+}$ and wild-type mice. Representative image of kidneys of 10 to 12 mice in each group. (**c**) Kidney planar surface area was calculated from photographed kidneys. (**d**) Increased kidney weight (KW) to body weight (BW) ratios were detected in all *cpk* mice compared to non-*cpk* mice, with *ErbB4*^{del}*ht*$^{+}$*-cpk* having the highest KW/BW ratio. In (c) and (d), values represent mean ± SE. n = 10 to 12 in each group. (**e**) Morphologically (H&E staining), cystic kidneys from *ErbB4*^{del}*ht*$^{+}$*-cpk* mice had severe cyst

formations and less remnant of renal cortex compared to the kidneys from *cpk* mice. (**f**) Cystic index, which represents the percentage of total area occupied by cysts, was significantly larger in *ErbB4*^{del}*ht*$^{+}$*-cpk* kidneys compared to *cpk* kidneys. (**g**) At P10, BUN levels in both *cpk* and *ErbB4*^{del}*ht*$^{+}$*-cpk* mice were significantly increased compared to controls, and BUN levels were further increased in *ErbB4*^{del}*ht*$^{+}$*-cpk* mice. n = 10 to 12 in each group.

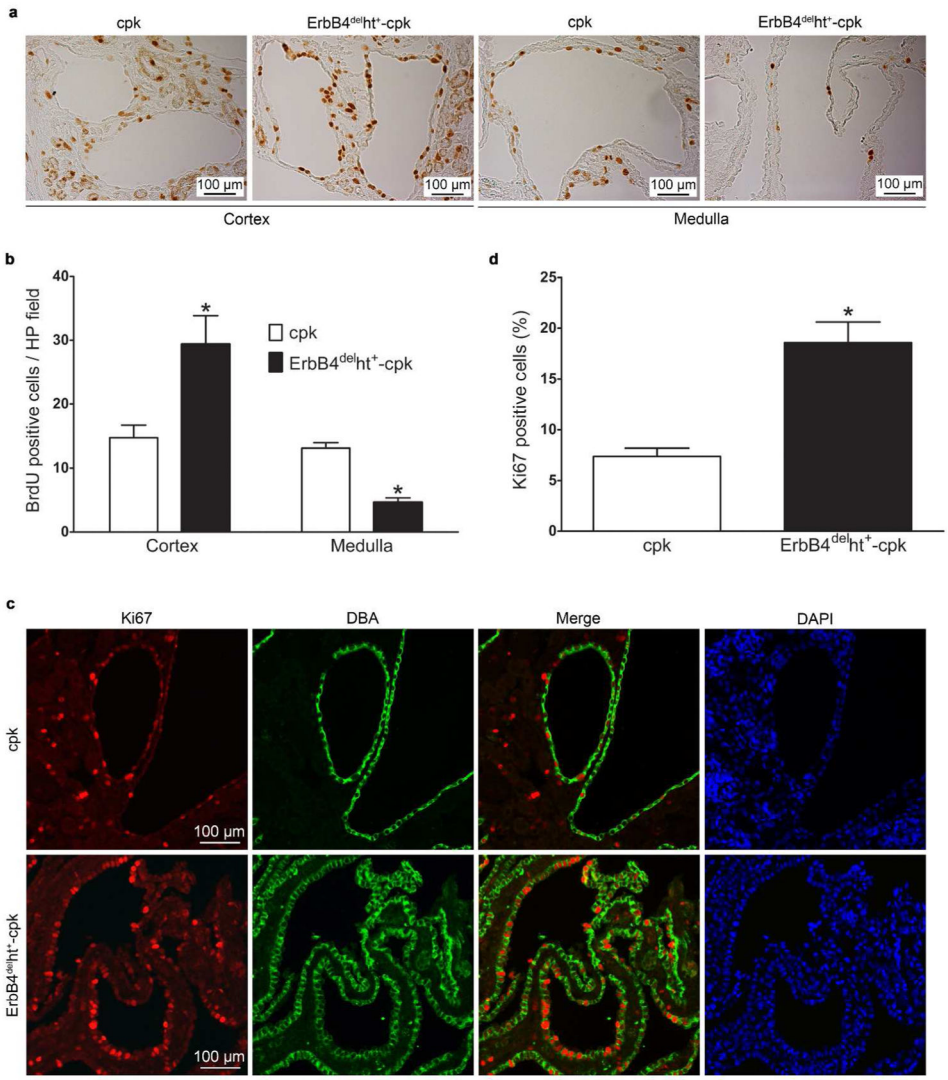

Figure 5.

Increased cell proliferation in the cyst-lining epithelial cells of *ErbB4*^{del}*ht*$^{+}$*-cpk* mice. (**a**) BrdU immunostaining (brown) showed that there were more proliferating cells in the cortex than medulla. (**b**) Quantification of BrdU positive cells along the cysts per high power field in (a). There were more BrdU positive cells along the cysts in the cortex, but less in the medulla, in *ErbB4*^{del}*ht*$^{+}$*-cpk* kidneys compared to *cpk* kidneys. **P* < 0.05 compared to *cpk*. (**c**) Ki67 (red) was double labeled with DBA, a collecting duct marker (green). Nuclei were stained with DAPI (blue). (**d**) Quantification of the Ki67 positive cells per cyst-lining epithelial cells in (c). **P* < 0.05.

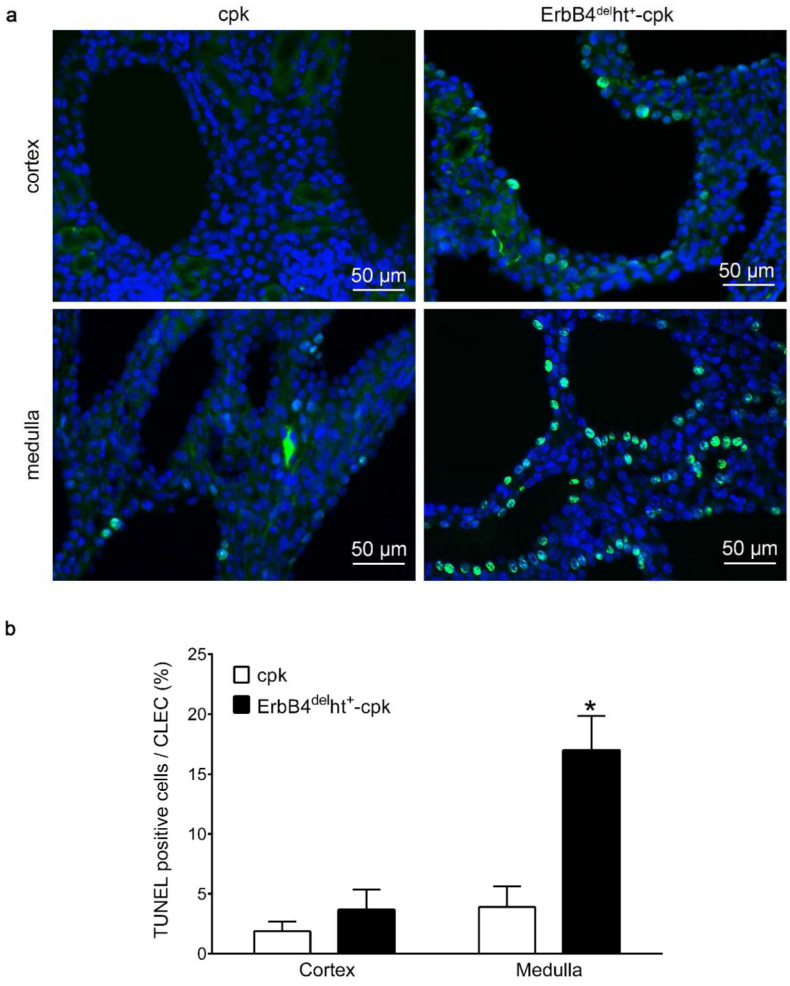

Figure 6.

Increased cell apoptosis in the cystic kidneys of *ErbB4^{del}ht^{+}-cpk* mice. (**a**) TUNEL labeling (green) was increased in cyst-formation cells of *ErbB4^{del}ht^{+}-cpk* kidneys compared to *cpk* kidneys. Compared to the cortex, more TUNEL labeled apoptotic cells were detected in the medulla. Nuclei were stained with DAPI (blue). (**b**) Quantification of the TUNEL labeling cells per cyst-lining epithelial cells (CLEC) in (a). *$P < 0.001$.

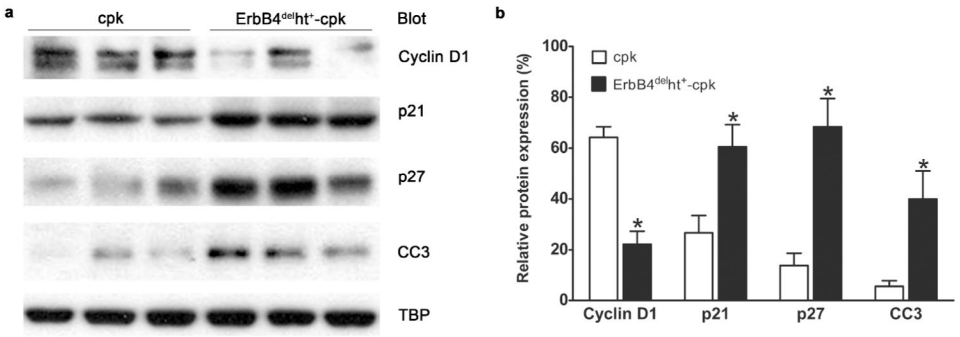

Figure 7.

Expression levels of cell-cycle regulatory proteins. (**a**) Western blots of nuclear extracts (30 μg) isolated from kidneys of P10 *ErbB4*^{del}*ht*$^{+}$*-cpk* and *cpk* mice. Decreased levels of cyclin D1 and increased levels of p21, p27 and cleaved caspase 3 (CC3) were detected in the kidneys from *ErbB4*^{del}*ht*$^{+}$*-cpk* compared to *cpk* mice. Equivalent amount of nuclear protein loading was confirmed by TATA binding protein (TBP) expression levels. (**b**) Densitometric analysis of the Western blot bands in (a) and expressed as their percentage to TBP. **P* < 0.05. Values represent mean ± SE of at least three independent experiments.

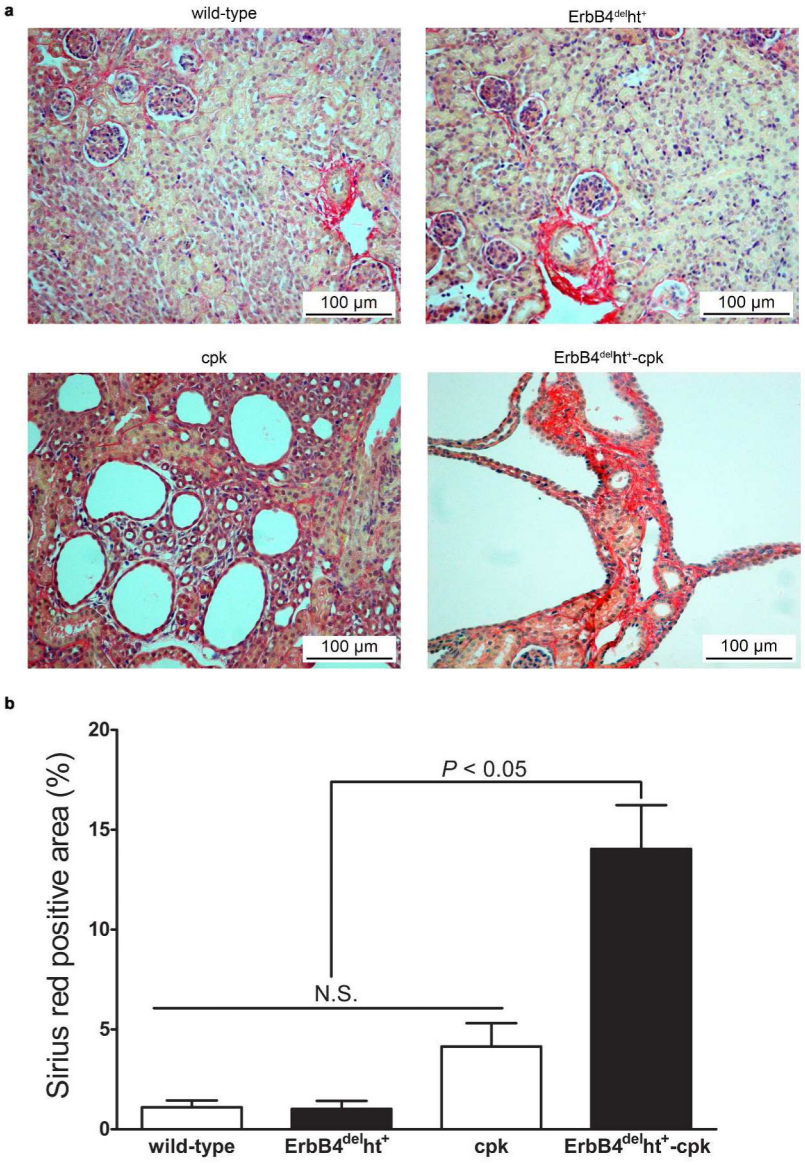

Figure 8.

Increased renal fibrosis in *ErbB4^{del}ht^{+}-cpk* kidneys. (**a**) Representative images of picosirius red staining on P10 kidneys from 10 to 12 mice in each group. (**b**) Using image J software, percentage of picosirius red area was calculated. There was significantly more fibrosis in *ErbB4^{del}ht^{+}-cpk* kidneys compared to all the other groups.